

## $Z_1^3$ -Dependent Stopping Power and Range Contributions\*

J. C. Ashley and R. H. Ritchie

Health Physics Division, Oak Ridge National Laboratory, Oak Ridge, Tennessee 37830

Werner Brandt

Department of Physics, New York University, New York, New York 10003

(Received 12 March 1973)

The theory of the  $Z_1^3$ -dependent contribution to the stopping of charged particles in matter is cast into simple formulas for stopping powers and range-energy relations which apply in a comprehensive manner to all targets. Formulas are given for compound targets and applied to the standard nuclear emulsion.

### I. $Z_1^3$ -DEPENDENT STOPPING-POWER CONTRIBUTIONS

The stopping power of a target composed of atoms with atomic number  $Z_2$ , for a projectile of atomic number  $Z_1$  and velocity  $v_1$ , depends in first Born approximation on the projectile charge as  $(Z_1 e)^2$ . Recently<sup>1,2</sup> we extended this theory to include the  $(Z_1 e)^3$  dependence in a classical treatment which is equivalent to a second Born approximation.<sup>3</sup> The  $Z_1^3$  contribution was calculated for the statistical model of the target atom in the Lenz-Jensen approximation. Expressing the projectile energy  $E_1$  in terms of the reduced parameter  $x \equiv v_1^2/v_0^2 Z_2 = 40.2 E_1$  (MeV)/ $M_1 Z_2$ , where  $v_0$  is the Bohr velocity and  $M_1$  the projectile mass in amu, we write the stopping power  $S(x)$  in terms of the stopping power in first Born approximation,<sup>4</sup>  $S_0(x)$ , in the form

$$S(x) = S_0(x) \left( 1 + \frac{Z_1}{Z_2^{1/2}} \frac{\kappa(b, x)}{x} \right). \quad (1)$$

Since  $S_0(x) \propto Z_2^2$ , the second term in the parentheses represents the  $Z_1^3$  contribution. In the statistical approximation, with the abbreviation  $b \equiv \chi \eta Z_2^{1/6}$ , the function  $\kappa(b, x)$  becomes

$$\kappa(b, x) = \frac{F(b/x^{1/2})}{x^{1/2} L(x)}, \quad (2)$$

where  $\chi \approx 1.3$  is a constant of the statistical model of the atom and  $\eta$  is related to the choice of the lower impact-parameter cutoff in the classical description. The function  $F(w)$  is derived and displayed in Ref. 2. The function  $L(x)$ , also derived and displayed in Ref. 2, is the stopping number per target electron; for  $x > 1$  we have

$$L(x) = \ln \left( \frac{2m_e v_1^2}{K_B Z_2} \right) = \ln \left( \frac{x}{q} \right), \quad (3)$$

where  $q = K_B/4\mathcal{R}$ .  $K_B$  denotes Bloch's constant

defined such that  $I_2(Z_2) = K_B Z_2$  is the mean excitation energy for stopping, and  $\mathcal{R} = 13.6$  eV. As discussed presently,  $K_B$  varies slowly with  $Z_2$ .<sup>5</sup> For application of Eq. (3), a value  $q = 0.18$  gives good agreement with the statistical model when  $x > 1$ . When  $x \leq 1$ , inner-shell corrections to Eq. (3) appear which we have taken into account in a statistical approximation.<sup>2</sup>

The oscillator-strength distribution in real atoms is always shifted to higher frequencies, with decreasing  $Z_2$ , compared with that of the statistical atom.<sup>6</sup> Therefore,  $\eta$  has a weak  $Z_2$  dependence similar to that of Bloch's constant,<sup>2</sup> viz.,  $\eta = \eta_0(1.23 + 0.717 Z_2^{-1})$  for  $Z_2 < 13$  and  $\eta = \eta_0(1 + 6.02 Z_2^{-1.19})$  for  $Z_2 \geq 13$ , where  $\eta_0$  is a constant of order unity. With this trend in  $\eta$ , the product  $\eta Z_2^{1/6}$  becomes practically independent of  $Z_2$ . Quantitatively,  $\eta Z_2^{1/6} = (2.0 \pm 0.2) \eta_0$  for  $1 \leq Z_2 \leq 100$ . This fact makes  $b$  in Eq. (1) a constant for all target elements.<sup>7</sup> Comparison with the available two sets of experiments<sup>8</sup> on Al ( $Z_2 = 13$ ) and Ta ( $Z_2 = 73$ ) yields the presently "best" trial value,  $b = 1.8 \pm 0.2$ . The function  $\kappa(b, x)/x$  versus  $x$  and compares it, according to Eq. (1), with the data<sup>8</sup> on Al and Ta in the form  $Z_2^{1/2} \Delta S(x)/Z_1 S_0(x) \equiv Z_2^{1/2} (S - S_0)/Z_1 S_0$ .

We note from Table I that  $\kappa(b, x)$  is a very slowly varying function of  $x$ . For many applications, at  $x > 1$ , it suffices to set  $\kappa$  equal to a mean constant,  $\kappa_0 \approx 0.32$ , because when  $x > 10$ , the  $Z_1^3$  contribution normally is too small to be retained, and deviations of  $\kappa$  from  $\kappa_0$  become irrelevant.

The  $Z_1^3$  contribution accounts for the shorter ranges of positive particles (e.g.,  $\pi^+$ ) compared to the ranges of their antiparticles ( $\pi^-$ ).<sup>2</sup> Most of these observations are made in nuclear emulsions.<sup>9</sup> We derive the  $Z_1^3$  contribution for a compound target under the assumption that Bragg's additivity rule of stopping power applies.<sup>10</sup> For a target consisting of atomic constituents  $Z_{2i}$ , present

in atomic concentrations  $n_i$ , the stopping power becomes  $S_0 = \sum n_i S_{0i}(x_i) / \sum n_i$ , where  $x_i \equiv v_1^2 / v_0^2 Z_{2i}$ .  $S_0$  and the corresponding range  $R_0$  are tabulated for many compounds.<sup>4,11</sup> Noting that  $S_{0i} \propto L(x_i) / x_i$ , the  $Z_1^3$  contribution takes the form

$$\frac{S - S_0}{S_0} \equiv \frac{\Delta S}{S_0} = Z_1 \left( \frac{v_0}{v_1} \right)^2 \frac{\sum n_i Z_{2i}^{3/2} L(x_i) \kappa(b, x_i)}{\sum n_i Z_{2i} L(x_i)} \quad (4)$$

With  $\kappa(b, x_i) \approx \kappa_0$ , Eq. (4) reduces to the convenient formula

TABLE I. Function  $\kappa(b, x)$  [Eq. (2)] for the parameter values  $b = 1.8 \pm 0.2$ .

$x$	$b = 1.6$	$b = 1.8$	$b = 2.0$
0.115	0.1944	0.1331	0.095 11
0.165	0.2161	0.1478	0.1052
0.215	0.2363	0.1620	0.1153
0.265	0.2544	0.1754	0.1251
0.315	0.2706	0.1877	0.1343
0.365	0.2851	0.1990	0.1431
0.415	0.2980	0.2095	0.1513
0.465	0.3095	0.2191	0.1590
0.515	0.3198	0.2279	0.1662
0.565	0.3290	0.2360	0.1729
0.615	0.3373	0.2434	0.1793
0.665	0.3447	0.2503	0.1852
0.715	0.3514	0.2566	0.1908
0.765	0.3575	0.2625	0.1960
0.815	0.3629	0.2679	0.2009
0.865	0.3679	0.2729	0.2055
0.915	0.3724	0.2774	0.2099
0.965	0.3765	0.2818	0.2139
1.	0.3792	0.2846	0.2166
1.3	0.3967	0.3043	0.2361
1.7	0.4081	0.3201	0.2534
2	0.4123	0.3277	0.2626
3	0.4134	0.3389	0.2794
4	0.4064	0.3396	0.2854
5	0.3970	0.3364	0.2865
6	0.3871	0.3316	0.2853
7	0.3774	0.3260	0.2829
8	0.3682	0.3203	0.2798
9	0.3596	0.3146	0.2763
10	0.3514	0.3090	0.2727
13	0.3304	0.2938	0.2622
17	0.3072	0.2760	0.2489
20	0.2930	0.2647	0.2400
30	0.2578	0.2359	0.2166
40	0.2337	0.2154	0.1993
50	0.2157	0.1999	0.1859
60	0.2016	0.1876	0.1751
70	0.1901	0.1774	0.1661
80	0.1806	0.1689	0.1586
90	0.1724	0.1616	0.1520
100	0.1653	0.1553	0.1463

$$\frac{\Delta S}{S_0} = \frac{Z_1}{Z_c^{1/2}} \frac{\kappa_0}{x_c} f(Z_c, x_c), \quad (5)$$

where for the compound target (subscript  $c$ )

$$f(Z_c, x_c) = \frac{Z_c^{1/2}}{Z_c^{1/2}} \left( 1 + \frac{\ln(\bar{Z}_c / \bar{Z}_c')}{L(x_c)} \right), \quad (6)$$

with the abbreviations

$$Z_c^{1/2} = \frac{\sum n_i Z_{2i}^{3/2}}{\sum n_i Z_{2i}}, \quad (7)$$

$$\ln \bar{Z}_c = \frac{\sum n_i Z_{2i} \ln Z_{2i}}{\sum n_i Z_{2i}}, \quad (8)$$

$$\ln \bar{Z}_c' = \frac{\sum n_i Z_{2i}^{3/2} \ln Z_{2i}}{\sum n_i Z_{2i}^{3/2}}, \quad (9)$$

$$x_c = v_1^2 / v_0^2 \bar{Z}_c. \quad (10)$$

For illustration we have evaluated Eq. (4) for the important case of standard emulsion for which  $S_0$  is tabulated.<sup>11-13</sup> In units of  $10^{20}$  atoms/cm<sup>3</sup>, it is defined by  $n_1 = 321.56$  (the index denotes the atomic number of the element; here  $Z_2 = 1$  for H),  $n_6 = 138.30$ ,  $n_7 = 31.68$ ,  $n_8 = 94.97$ ,  $n_{16} = 1.353$ ,  $n_{35} = 100.41$ ,  $n_{47} = 101.01$ , and  $n_{53} = 0.565$ .<sup>11,12</sup> The result is plotted as the solid curve in Fig. 2, in the form  $\beta^2 \Delta S(\beta) / Z_1 S_0(\beta)$  versus  $\beta \equiv v_1 / c = \alpha [40.2 E_1 (\text{MeV}) / M_1]^{1/2}$ , where  $\alpha \equiv v_0 / c = 1/137$ . We find a difference of 6.3% in the emulsion stopping power

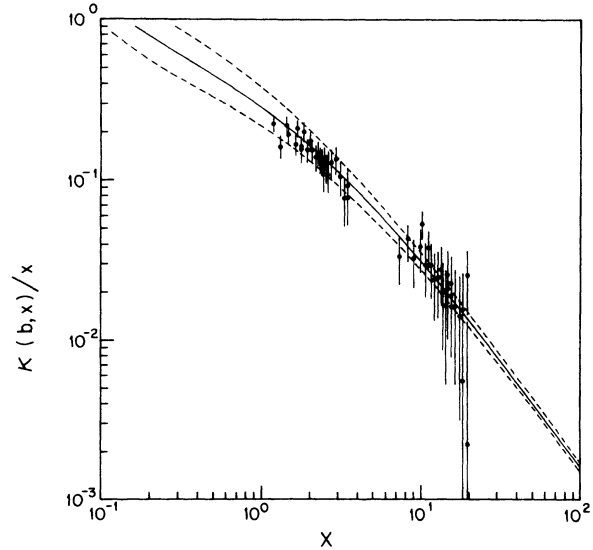


FIG. 1. Comparison of  $\kappa(b, x)/x$  [Eq. (1)] for  $b = 1.8$  (solid curve) with experiments by Andersen, Simonsen, and Sørensen, (Ref. 8.) The upper and lower dashed curves correspond to 10% changes in  $b$ , viz.,  $b = 1.6$  and  $b = 2.0$ , as tabulated in Table I. The group of data near  $x = 2$  comes from measurements on a Ta ( $Z_2 = 73$ ) target, the group near  $x = 10$  from measurements on an Al ( $Z_2 = 13$ ) target.

for  $\pi^+$  versus  $\pi^-$  at 1.2 MeV/amu, a value slightly smaller than the tentative estimate of 8–9% given in Ref. 2. The approximate Eq. (5), with the parameter values listed in Table II, is shown as the dashed curve in Fig. 2.

We make contact with Eq. (1) by *ex post facto* replacing  $\kappa_0$  in Eq. (5) with  $\kappa(b, x_c)$  as tabulated in Table I. This then yields the stopping-power formula for compounds:

$$S(x_c) = S_0(x_c) \left( 1 + \frac{Z_1}{Z_2^{1/2}} \frac{\kappa(b, x_c)}{x_c} f(Z_2, x_c) \right). \quad (11)$$

We illustrate in Fig. 2 the equivalence of Eq. (11) (dot-dash curve) with the exact equation (4) (solid curve). For elemental targets, Eq. (11) reduces to Eq. (1).

The  $Z_1^3$  contribution was recently extended to the stopping power of heavy ions by Kelley *et al.*<sup>14</sup> As a first approximation to a description of this situation we simply replace  $Z_1$  by an effective charge for the heavy ion. If  $S_0(x, Z_1)$  is taken to be the "best" theoretical  $Z_1^2$  stopping power of the ions (i.e., with no  $Z_1^3$  contribution), Eq. (1) can be written in the form

$$S(x, Z_1) = S_0(x, Z_1) \times \left( 1 + \frac{q_{1\text{eff}}(v_1/v_0, Z_1)}{Z_1} \frac{Z_1}{Z_2^{1/2}} \frac{\kappa(b, x)}{x} \right), \quad (12)$$

which applies as long as  $q_{1\text{eff}} \ll Z_2^{1/2} x / \kappa_0$ . In terms of the probability  $m_i(v_1/v_0, Z_1)$  that the ion

of atomic number  $Z_1$  and velocity  $v_1$  is in the charge state  $q_{1i}$ , we have

$$\frac{q_{1\text{eff}}(v_1/v_0, Z_1)}{Z_1} = \frac{\sum_{i=0}^{Z_1} m_i(v_1/v_0, Z_1) q_{1i}^3}{Z_1 \sum_{i=0}^{Z_1} m_i(v_1/v_0, Z_1) q_{1i}^2}. \quad (13)$$

The effective charge state for the stopping power in dense targets is known to be essentially independent of  $Z_2$ , so that the substitution of  $q_{1\text{eff}}$  for  $Z_1$  in Eq. (12) applies also to compounds, provided  $q_{1\text{eff}} \ll Z_2^{1/2} x_c / \kappa(b, x_c)$ . The distribution of  $m_i$  can be assumed to be sufficiently narrow for us to set  $\langle q_{1i}^3 \rangle = \langle q_{1i}^2 \rangle^{3/2}$ . The function  $q_{1\text{eff}}(v_1/v_0, Z_1)$  [Eq. 13] is then equal to  $\langle q_{1i}^2 \rangle^{1/2}$  as determined from stopping-power measurements. Best fits to existing data<sup>15,16</sup> can be summarized in the form

$$\frac{q_{1\text{eff}}(v_1/v_0, Z_1)}{Z_1} = 1 - C e^{-v_1/v_0 \gamma(Z_1)}, \quad (14)$$

where

$$C = 1.0, \quad \gamma(Z_1) = \frac{1}{2}(Z_1 - 0.35) \quad \text{for } 4 < Z_1 \leq 10 \text{ and } (v_1/v_0) > 0.25 Z_1; \quad (15a)$$

$$C = 1.032, \quad \gamma(Z_1) = Z_1^{0.69} \quad \text{for } Z_1 \geq 35 \text{ and } (v_1/v_0) > 0.1 Z_1^{0.69}. \quad (15b)$$

The analysis of the stopping-power data for C, N, and O in silicon by Kelley *et al.*<sup>14</sup> along these lines agrees with Eqs. (12), (14), and (15a).

In light of Eq. (1), presently available precision values of the mean excitation energy for stopping,  $I'_2$ , must be corrected to obtain the excitation energy  $I_2$ , central to the first-Born-approximation stopping-power theory, as it appears in Eq. (3). Specifically, for  $x > 1$ , we have

$$I_2 \approx I'_2 \left( 1 + \frac{Z_1}{Z_2^{1/2}} \frac{\kappa(b, x)}{x} L(x) \right). \quad (16)$$

$I_2$  values, so derived from experiment, will have

TABLE II. Parameters of standard nuclear emulsion, as defined in the text, for use in  $Z_1^3$  contributions to stopping powers [Eqs. (5) and (6)] and to ranges [Eqs. (22) and (23)].

$Z_1^{1/2} = 5.62$	$q = 0.18$
$\bar{Z}_c = 27.06$	$Q \text{ (MeV)} = 0.1234 M_1 \text{ (amu)}$
$\bar{Z}_c' = 35.47$	$I_2 = 270 \text{ eV}$
$\ln(\bar{Z}_c/\bar{Z}_c') = -0.2706$	$E_1 \text{ (MeV)}$
$\kappa_0 = 0.32 \pm 0.05$	$\eta = 0.59$
$x_c = 1.49 E_1 \text{ (MeV)} / M_1 \text{ (amu)}$	

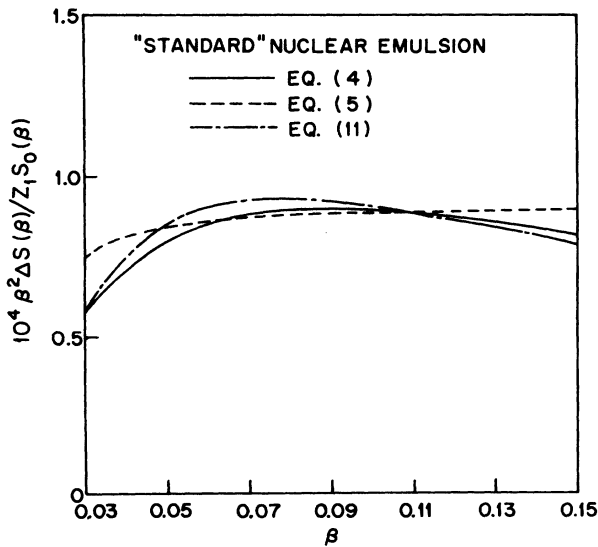


FIG. 2.  $Z_1^3$  effect on the stopping power of a compound [Eq. (4)] as applied to the standard emulsion (solid curve). The dashed line represents Eq. (5) with the coefficients listed in Table II. The dot-dash curve depicts Eq. (11) for  $b = 1.8$ .

a somewhat different  $Z_2$  dependence than the  $I_2'$  values known at present. Practical implications aside, this will bear on the experimental tests of the theory of  $K_B$  and of inner-shell corrections.

## II. $Z_1^3$ -DEPENDENT RANGE CONTRIBUTIONS

With Eq. (1) the range  $R(x)$ , including the  $Z_1^3$  contribution, becomes

$$R(x) = \int^x \left( \frac{M_1 \mathcal{R} Z_2}{m} \right) \frac{dx'}{S(x')} = R_0(x) \left[ 1 - \frac{Z_1}{Z_2^{1/2} R_0(x)} \int^x \frac{\kappa(b, x')}{x' S_0(x')} \left( \frac{M_1 \mathcal{R} Z_2}{m} \right) dx' \right] \approx R_0(x) \left( 1 - \frac{Z_1 \kappa_0}{Z_2^{1/2}} \frac{r_0(x)}{R_0(x)} \right), \quad (17)$$

where  $R_0$  are tabulated theoretical ranges.<sup>4,11,13,17,18</sup> In the last expression,  $\kappa(b, x)$  is approximated by  $\kappa_0$ ;  $r_0(x)$  denotes the integral

$$r_0(x) = \int^x \left( \frac{M_1 \mathcal{R} Z_2}{m} \right) \frac{dx'}{x' S_0(x')}. \quad (18)$$

For  $x > 1$  Eq. (3) dominates the range integration. Then, since  $S_0(x) \propto x^{-1} \ln(x/q)$ , Eq. (18) obeys the transformation

$$q r_0(x) = R_0((qx)^{1/2}), \quad (19)$$

so that Eq. (17) reduces to the simple form

$$R = R_0(x) \left( 1 - \frac{Z_1 \kappa_0}{Z_2^{1/2} q} \frac{R_0((qx)^{1/2})}{R_0(x)} \right) = R_0(E_1) \left( 1 - \frac{4 Z_1 \kappa_0 \mathcal{R}}{Z_2^{1/2} K_B} \frac{R_0((QE_1)^{1/2})}{R_0(E_1)} \right), \quad (20)$$

in terms only of known ranges  $R_0$ . The constant  $\kappa_0/q$  has the value  $\approx 1.78$ . In the last version,  $E_1$  is given in MeV, and  $Q$  (MeV) =  $4.57 \times 10^{-4} M_1$  (amu)  $I_2$  (eV).

It is well established, over wide intervals of  $E_1$ ,

that the range-energy relation can be approximated accurately by  $R_0 = (E_1/k)^{1/\eta}$ , where  $k$  is a constant and  $\eta(E_1)$  is the range-energy index which is tabulated.<sup>13</sup> For  $5 \leq E_1$  (MeV)/ $M_1 \leq 200$ ,  $\eta(E_1)$  varies only very slowly and has a mean value close to  $\eta = 0.6$  [compared to Geiger's rule  $\eta_G = 2/3$ , applicable to the low energies of natural  $\alpha$  particles corresponding to  $(E_1/M_1) \approx (1-2)$  MeV/amu]. Then we have

$$R = R_0(x) \left[ 1 - \frac{Z_1 \kappa_0}{Z_2^{1/2} q} \left( \frac{q}{x} \right)^{1/2 \eta} \right] = R_0(E_1) \left[ 1 - \frac{4 Z_1 \kappa_0 \mathcal{R}}{Z_2^{1/2} K_B} \left( \frac{Q}{E_1} \right)^{1/2 \eta} \right] \quad (21)$$

in the notation of Eq. (20). The effect of the slow variation of  $\kappa$  with  $x$  can be incorporated approximately by replacing  $\kappa_0$  in Eq. (21) with  $\kappa(b, x)$  and, in the following range formulas for compounds, with  $\kappa(b, x_c)$ .

Range formulas for compounds, including the  $Z_1^3$  contribution, follow directly from Eq. (17), using Eqs. (5), (6), (19), and the definitions in Eqs. (7)–(9). For  $E_1$  in MeV, the result is<sup>19</sup>

$$R(E_1) = R_0(E_1) \left\{ 1 - \frac{Z_1 Z_c^{1/2}}{Z_c} \frac{\kappa_0}{q} \left[ \frac{R_0((QE_1)^{1/2})}{R_0(E_1)} \left( 1 + \ln \frac{Z_c}{Z_c'} \right) - \frac{Q \ln(Z_c/\bar{Z}_c')}{S_0(E_1) R_0(E_1)} \right] \right\}. \quad (22)$$

With  $R_0(E_1) = (E_1/k)^{1/\eta}$ , Eq. (22) simplifies to

$$R(E_1) = R_0(E_1) \left\{ 1 - \frac{Z_1 Z_c^{1/2}}{Z_c} \frac{\kappa_0}{q} \left[ \left( \frac{Q}{E_1} \right)^{1/2 \eta} \left( 1 + \ln \frac{Z_c}{Z_c'} \right) - \frac{Q}{\eta E_1} \ln \frac{Z_c}{Z_c'} \right] \right\}. \quad (23)$$

Equations (22) and (23) reduce to Eqs. (20) and (21) for elemental targets. With the aid of tables of  $S_0(E_1)$  and  $R_0(E_1)$ ,<sup>4,11,13,17,18</sup> Eq. (22) is a convenient and accurate formula for calculating  $R(E_1)$ , or for constructing curves of  $(R - R_0)$  versus  $R_0$  by using  $E_1$  from tables of  $R_0(E_1)$  as the connecting parameter, or for pairs of antiparticles  $\Delta R = (R_- - R_+) = 2 |R - R_0|$  versus  $R_0$ . Equations (21) and (23) are somewhat less accurate, but useful for ready calculations when the range-energy

index  $\eta$  is known. Note that in calculating  $R$  from tabulated ranges and stopping powers care should be taken to use only theoretical values, since values derived from experiment will already contain a  $Z_1^3$  contribution. However, for calculating  $R - R_0$  and range differences between a particle and its antiparticle, values of  $S_0$  and  $R_0$  derived from experiment may be used, since the inclusion of a  $Z_1^3$  contribution in  $S_0$  and  $R_0$  here will produce only a small higher-order contribution to the

range differences.

We have performed calculations of  $\Delta R$  for  $\pi^-$  versus  $\pi^+$  as a function of  $R_0$  in nuclear emulsion from Eq. (22), using Tables II and III of Ref. 13, and from Eq. (23). The constants for nuclear emulsion were taken from Table II. The results are shown graphically in Fig. 3. Slightly lower values are found from the expedient formulas [Eqs. (21) and (23)] compared to the results of the more accurate equations (20) and (22), as a consequence of employing the value of the range-energy index  $\eta$ , appropriate for  $E_1$ , for both  $R_0$  ( $(QE_1)^{1/2}$ ) and  $R_0(E_1)$ . The results calculated with the analytical formulas agree quite well with the results found in Ref. 7 by numerical integration. The values estimated from Fig. 4 in Ref. 7 are shown as cross marks in Fig. 3. The small difference in the results at the higher energies is due to relativistic corrections which are not included in our analytical formulas.

The theoretical  $\Delta R_\pi$  values from Eq. (22) are about 40% smaller than the range differences measured by Barkas *et al.*<sup>20</sup> at the  $\pi^+$  ranges 80 and 90  $\mu\text{m}$ . The theoretical value  $\Delta R_\pi = 1.69$  at  $R_{\pi^+} = 80 \mu\text{m}$  (see Fig. 3) agrees satisfactorily with the recent measurement  $\Delta R_\pi = (2.0 \pm 0.3) \mu\text{m}$  by Tovee *et al.*<sup>21</sup> At  $R_{\pi^+} = 725 \mu\text{m}$ , the theoretical

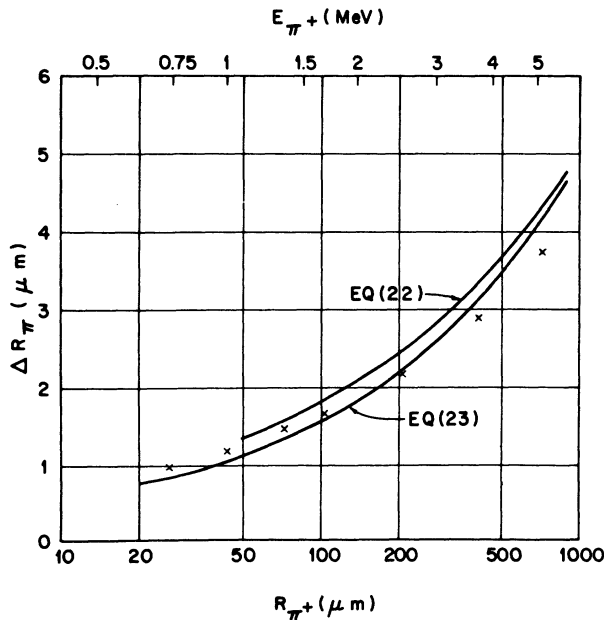


FIG. 3. Range difference for  $\pi^+$  and  $\pi^-$  mesons in nuclear emulsion,  $\Delta R_\pi \equiv R_{\pi^-} - R_{\pi^+}$ , as a function of  $R_{\pi^+}$  and  $E_{\pi^+}$ , calculated according to Eqs. (22) and (23) with the constants listed in Table II and range-energy tables given in Ref. 13. The cross marks are estimates of the range difference derived from results presented in Ref. 7.

value  $\Delta R_\pi = 4.35 \mu\text{m}$  agrees, within the uncertainties, with the measured value  $\Delta R_\pi = (5.5 \pm 3.2) \mu\text{m}$  reported by Barkas *et al.*<sup>20</sup>

### III. USE OF TABLES

Extensive tables of the functions  $F, L$ , and of the central function  $I(\xi)$  defined in Ref. 2 can be obtained from the National Auxiliary Publication Service.<sup>22</sup> From these tables, with Eq. (2), the function  $\kappa(b, x)$  for parameter values not listed in Table I can be calculated readily.

### ACKNOWLEDGMENT

The authors are grateful to V. E. Anderson for his careful work in evaluating numerically the functions used here.

### APPENDIX: APPLICATIONS

In the following appendix we present in detail three examples illustrating the use of the formulas derived in this paper for the calculation of  $Z_1^3$  contributions to stopping power and range. For practical applications one should be aware that the tabulated theoretical stopping powers and ranges are to some extent uncertain owing to uncertainties in mean excitation energies, shell corrections, nonadditivity in the case of compounds, etc. Thus, the addition of the  $Z_1^3$  contribution may or may not be meaningful, depending on the size of the  $Z_1^3$  contribution compared with the uncertainty in the theoretical stopping-power or range values. In the examples we do not consider these questions, but simply provide the examples as guides to the use of the analytic formulas.

#### A. Example (i): Stopping Power of 8-MeV $\alpha$ Particle in Water ( $\text{H}_2\text{O}$ )

*Procedure.* Use, e.g., Eq. (11). Calculate the target constants  $Z_c^{1/2}$ ,  $\bar{Z}_c$ , and  $\ln(\bar{Z}_c/Z_c')$  according to Eqs. (7)–(9) and  $x_c = 40.2E_1(\text{MeV})/M_1(\text{amu})\bar{Z}_c$ . Then  $f(Z_c, x_c) = (Z_c^{1/2}/\bar{Z}_c^{1/2}) \{1 + [\ln(\bar{Z}_c/Z_c')]/L(x_c)\}$  by Eq. (6), with  $L(x_c) = \ln(x_c/q)$  by Eq. (3). [If  $x_c \lesssim 1$ , Eq. (3) does not apply; instead, read  $L(x_c)$  from Fig. 3 in Ref. 2 or from the tables in Ref. 22.] Determine  $\kappa(1.8, x_c)$  from Table I. [Note that the value  $b = 1.8$  should be used as long as the present data and new data confirm the curve in Fig. 1. If changes are necessary, read  $\kappa(b, x)$  for the new  $b$  from Table I by interpolation between  $b = 1.6$  and  $b = 1.8$ ] Calculate the term  $[1 + Z_1 f(Z_c, x_c) \kappa(b, x_c) / \bar{Z}_c^{1/2} x_c]$  and multiply with the best-tabulated stopping power for this particle-target combination at  $E_1$  to obtain the

stopping power, including the  $Z_1^3$  contribution.

*Results.* For water of density  $n_0$  molecules per unit volume, the hydrogen-atom density is  $n_1 = 2n_0$  and the oxygen-atom density is  $n_8 = n_0$ , so Eqs. (7)–(9) give  $Z_c^{1/2} = [(2)(1^{3/2}) + (1)(8^{3/2})] / [(2)(1) + (1)(8)] = 2.4627$ ,  $\ln \bar{Z}_c = [(1)(8) \ln 8] / [(2)(1) + (1)(8)] = 1.6636$ , and  $\ln \bar{Z}'_c = [(1)(8^{3/2}) \ln 8] / [(2)(1^{3/2}) + (1)(8^{3/2})] = 1.9106$ . Thus,  $\bar{Z}_c = 5.278$  and  $\ln(\bar{Z}_c / \bar{Z}'_c) = -0.2470$ . Also,  $x_c = (40.2)(8) / (4)(5.278) = 15.2$ , so with  $q = 0.18$ ,  $L(15.2) = \ln(15.2/0.18) = 4.44$ . With these values,  $f(Z_c, x_c) = (2.463/2.297) \times [1 + (-0.2470)/(4.44)] = 1.01$ . From Table I  $\kappa(1.8, 15.2) = 0.2840$  by linear interpolation. Thus we have  $[1 + Z_1 f(Z_c, x_c) \kappa(1.8, x_c) / \bar{Z}_c^{1/2} x_c] = [1 + (2)(1.01)(0.284)/(2.30)(15.2)] = 1.016$ , or a contribution to the stopping power of 1.6%.

#### B. Example (ii): Range of 16-MeV Proton in Aluminum

*Procedure.* Use, e.g., Eq. (20). Calculate  $QE_1 = 4.57 \times 10^{-4} M_1$  (amu)  $I_2$  (eV)  $E_1$  (MeV). From a table of calculated ranges find  $R_0(E_1)$  and  $R_0((QE_1)^{1/2})$ , and with  $\kappa_0/q = 1.78$  calculate the factor  $[1 - Z_1(\kappa_0/q)R_0((QE_1)^{1/2})/Z_1^{1/2}R_0(E_1)]$ . The tabulated theoretical range multiplied by this factor gives the range including the  $Z_1^3$  contribution.

*Results.* For Al with  $I_2 = 166$  eV,  $QE_1 = (4.57 \times 10^{-4})(1)(166)(16) = 1.214$  (MeV)<sup>2</sup>. From a table of proton ranges in aluminum (Ref. 18, p. 8-161), we find  $R_0(16\text{-MeV } p) = 0.3879$  g/cm<sup>2</sup> and

$$\begin{aligned} \Delta R &= 2 \frac{Z_1 Z_c^{1/2}}{Z_c} \frac{\kappa_0}{q} \left[ R_0((QE_1)^{1/2}) \left( 1 + \ln \frac{Z_c}{Z'_c} \right) - \frac{Q \ln(\bar{Z}_c / \bar{Z}'_c)}{S_0(E_1)} \right] \\ &= 2 \frac{(1)(5.62)(0.32)}{(27.06)(0.18)} \left( (2.50)(1 - 0.2706) - \frac{(0.01849)(-0.2706)}{107 \times 10^{-4}} \right) \\ &= 1.69 \text{ } \mu\text{m}. \end{aligned}$$

This value of  $\Delta R_\pi$  for the theoretical range 80  $\mu\text{m}$  compares well with the value  $2.0 \pm 0.3 \text{ } \mu\text{m}$  obtained

$R_0((QE_1)^{1/2}) = R_0(1.102\text{-MeV } p) = 0.0048$  g/cm<sup>2</sup>. Thus, with  $Z_1 = +1$ , the factor is  $[1 - (1)(1.78) \times (0.0048)/(13^{1/2})(0.3879)] = 0.994$ , and the range for a 16-MeV proton in aluminum, including the  $Z_1^3$  contribution, becomes  $R(16\text{-MeV } p) = (0.3879) \times (0.994) = 0.3856$  g/cm<sup>2</sup>.

#### C. Example (iii): Range Difference Due to $Z_1^3$ Effect Between $\pi^+$ and $\pi^-$ Mesons for Theoretical Pion Range of 80 $\mu\text{m}$ in Emulsion

*Procedure.* Use, e.g., Eq. (22). Find the energy  $E_1$  corresponding to the given range from tables of calculated ranges. The constants for standard emulsion are found in Table II. Calculate for emulsion  $Q$  (MeV)  $= 0.1234 M_1$  (amu) and  $(QE_1)^{1/2}$ . From tables, find  $S_0(E_1)$  and  $R_0((QE_1)^{1/2})$ . The range difference is given by  $\Delta R = 2 |R - R_0|$ .

*Results.* The energy of a  $\pi$  meson with a theoretical range of 80  $\mu\text{m}$  is  $E_1 = 1.448$  MeV by linear interpolation from Table III of Ref. 13.  $M_1(\pi) = 0.14985$  amu, so  $Q = (0.1234)(0.14985) = 0.01849$  MeV and  $(QE_1)^{1/2} = [(0.01849)(1.448)]^{1/2} = 0.1636$  MeV. From Ref. 13, Table III,  $R_0((QE_1)^{1/2}) = 2.50 \text{ } \mu\text{m}$  by interpolation.  $S_0(E_1)$  for  $\pi$  is the same as  $S_0$  for an equal-velocity proton, so a 1.448-MeV  $\pi$  has the same  $S_0$  as a proton of energy  $[M_1(\text{proton})/M_1(\pi)](1.448) = 9.73$  MeV. From Ref. 13, Table II,  $S_0(1.448) = 107 \times 10^{-4}$  MeV/ $\mu\text{m}$ . With the emulsion constants from our Table II, we have

by Tovee *et al.*<sup>21</sup> for the experimental range  $R_{\pi^+} = 80 \text{ } \mu\text{m}$ .

\*Research sponsored in part by the U. S. Atomic Energy Commission under contract with the Union Carbide Corporation.

<sup>1</sup>J. C. Ashley, W. Brandt, and R. H. Ritchie, *Bull. Am. Phys. Soc.* **15**, 1338 (1970).

<sup>2</sup>J. C. Ashley, R. H. Ritchie, and W. Brandt, *Phys. Rev. B* **5**, 2393 (1972).

<sup>3</sup>K. W. Hill and E. Merzbacher [*Bull. Am. Phys. Soc.* **16**, 1349 (1971); and private communication] have demonstrated that in the harmonic-oscillator approximation our classical results are identical with those of the

quantum-mechanical treatment.

<sup>4</sup>Cf., e.g., *Studies in Penetration of Charged Particles in Matter* (National Academy of Sciences-National Research Council, Washington, D. C., 1964, Publ. No. 1133), and references cited therein.

<sup>5</sup>Reference 4, p. 115.

<sup>6</sup>W. Brandt and S. Lundqvist, *Phys. Rev.* **139**, A612 (1965).

<sup>7</sup>J. D. Jackson and R. L. McCarthy [*Phys. Rev. B* **6**, 4131 (1972)] have repeated our treatment for a somewhat different small impact-parameter cutoff and arrive at

- the same conclusion. Therefore, their Fig. 1 contains a display essentially of the function  $\kappa(b, x)$  as given in Table I.
- <sup>8</sup>H. H. Andersen, H. Simonsen, and H. Sørensen, Nucl. Phys. A125, 171 (1969).
- <sup>9</sup>H. H. Heckman and P. J. Lindstrom, Phys. Rev. Lett. 22, 871 (1969), and references cited therein.
- <sup>10</sup>W. Brandt, Health Phys. 1, 11 (1958).
- <sup>11</sup>W. Brandt, *Energy Loss and Range of Charged Particles in Compounds*, Dupont Research Report 1960. NAPS Document No. 02194, to be ordered from ASIS NAPS, c/o Microfiche Publications, 305 E. 46th St., New York, N.Y. 10017, remitting \$1.50 for microfiche or \$5.00 for photocopies up to 30 pages and \$0.15 per each additional page over 30. Estimate 50 pages.
- <sup>12</sup>W. H. Barkas, Nuovo Cimento 8, 201 (1958).
- <sup>13</sup>M. M. Shapiro, in *Handbuch der Physik*, edited by S. Flügge (Springer-Verlag, Heidelberg, 1958), Vol. 45, p. 361ff.
- <sup>14</sup>J. G. Kelley, B. Sellers, and F. A. Hanser (unpublished).
- <sup>15</sup>L. C. Northcliff, Phys. Rev. 120, 1744 (1960).
- <sup>16</sup>H. D. Betz, Rev. Mod. Phys. 44, 465 (1972), Fig. 5.30.
- <sup>17</sup>C. F. Williamson, J. P. Boujot, and J. Picard, Tables of Range and Stopping Power of Chemical Elements for Particles of Energy 0.5 to 500 MeV, Saclay Report No. R3042, 1966 (unpublished).
- <sup>18</sup>H. Bichsel, in *American Institute of Physics Handbook*, 3rd edition (McGraw-Hill, New York, 1972), p. 8-142.
- <sup>19</sup>Making use of the approximate relation  $\int^x dx' L^{-2}(x') = \int^x dx' L^{-1}(x') - xL^{-1}(x)$ .
- <sup>20</sup>W. H. Barkas *et al.*, Phys. Rev. 101, 778 (1956); Phys. Rev. Lett. 11, 26 (1963); CERN Report No. 65-4 (unpublished).
- <sup>21</sup>D. N. Tovee *et al.*, Nucl. Phys. B 33, 493 (1971); and private communication.
- <sup>22</sup>J. C. Ashley, V. E. Anderson, R. H. Ritchie, and W. Brandt, *Z<sub>1</sub><sup>3</sup> Effect in the Stopping Power of Matter for Charged Particles: Tables of Functions*, NAPS Document No. 02195, to be ordered from ASIS NAPS, c/o Microfiche Publications, 305 E. 46th St., New York, N.Y. 10017, remitting \$1.50 for microfiche or \$5.00 for photocopy up to 30 pages and \$0.15 per each additional page over 30. Estimate 17 pages.